Hadamard Transform Techniques in Photothermal Spectroscopy

Patrick J. Treado and Michael D. Morris*
Department of Chemistry, The University of Michigan
Ann Arbor, Michigan 48109-1055

ABSTRACT

Hadamard transform imaging is shown to be generally applicable to any linear spectroscopy and to be useful where locally high power densities are undesirable. Application to transverse photothermal deflection and Raman spectroscopies is reviewed. The modulation transfer functions (MTF) of both source-encoded and signal-encoded Hadamard imagers are described. Preliminary results from a signal-encoded imager are presented.

INTRODUCTION

Hadamard transform imaging is a multiplexing technique that provides spatially resolved images from unfocused laser beams[1-6]. Because it operates with distributed light intensity, Hadamard imaging is advantageous for use with lasers whose peak or average power would otherwise damage samples. The method is a convenient alternative to the rastering and tight focusing employed in conventional laser microscopy, such as the Raman microprobe[7,8].

The need for laser power distribution is clear if pulsed lasers are employed. Even if CW lasers are employed, power density reduction remains important. A 50 mW beam tightly focused through a microscope objective can easily produce local temperature rises of 50°–100° in absorbing solids. While thermal decomposition or ablation is unlikely, melting or phase changes can easily occur.

There are two forms of Hadamard transform imaging. In source-encoded imaging, the signal is obtained by exciting the sample with a mask-encoded laser beam. In signal-encoded imaging, the sample is illuminated with an unfocused laser beam and the spectroscopic signal image is encoded by a series of Hadamard masks before presentation to a spectrometer.

Source-encoded Hadamard imaging is required where it is difficult or impossible to observe and manipulate an image of the analytical signal. Indirect absorption techniques, including transverse photothermal deflection spectroscopy (PDS) and photoacoustic spectroscopy (PAS) are important examples. In principle, source-encoded imaging is applicable to most spectroscopies. The only requirements are that the signals from the spatial elements of the sample be independent and that the detector generate the sum or weighted sum of the signals from illuminated spatial elements.

If the analytical signal can be imaged, as in Raman scattering, signal encoding is preferred. Signal encoding allows use of masking devices, such as photographic masks or spatial light modulators, which can not withstand high source intensities. Aperture diffraction is less severe, because the analytical signal from a coherent source is usually incoherent or only partially coherent.

We describe here the theory which describes both schemes, and the strengths and limitations of various experimental configurations in photothermal and Raman imaging. Photothermal imaging provides high sensitivity and is applicable to thin layer chromatography,[1-4] and to densitometry of protein blots. Raman imaging provides complete vibrational spectra at moderate sensitivity, with the potential for diffraction-limited spatial resolution.[5,6] The power distribution advantage of Hadamard techniques

may allow extension of Raman microscopy to pulsed laser excitation, which should prove extremely useful in ultraviolet resonance Raman studies of biological materials.

THEORY

Hadamard transform theory and application to spectroscopy and imaging have been reviewed.[9-11] The exciting laser beam or the signal from the illuminated sample is encoded with a series of n independent masks. Each mask is composed of a pseudo-random array of binary elements. The spatial distribution from the n resolution elements can be recovered from the set of n independent linear equations for the n mask configurations. In matrix notation, equation 1 describes the system.

$$\mathrm{Y} = \mathrm{S} \cdot \mathrm{X} \tag{1}$$

In equation 1, $\mathbf{Y}$ is a matrix consisting of the measured signals, y_i for the n mask configurations. $\mathbf{X}$ is a matrix representing the individual signals x_i for the n positions on the sample. The matrix S describes the configurations of the n masks and is called an S-matrix. S-matrices are derived from Hadamard matrices.[11] The decoded data can be recovered by equation 2.

$$\mathrm{X} = \mathrm{S}^{-1} \cdot \mathrm{Y} \tag{2}$$

Recovery of the data is facilitated if the number of elements encoded is $2^n - 1$. In these cases, the fast Hadamard transform (FHT) can be used, reducing the number of steps from $n^2 - n$ to $n\log_2 n$. Algorithms for constructing mask sequences and for generating fast Hadamard transforms have been published.[11]

Resolution of an imaging system is described by its modulation transfer function (MTF), which is a plot of image contrast versus spatial frequency.[12,13] We have presented approximate treatments of the modulation transfer function of a source-encoded Hadamard imaging system.[3,4] Here, we extend these arguments to the signal-encoded Hadamard imaging system. We describe contributions to the transfer function in a two-dimensional mask sequence of unit square aperture, d, using image magnification, M, to improve spatial resolution.

Equation 3 describes the effect of convolution with the finite width, d of the aperture.

$$MTF_a = \Lambda\left(\frac{f_x d}{M}\right) \tag{3}$$

In equation 3, Λ is the triangle function. The significance of this equation is that the magnified image is resolved to higher spatial frequencies than the inverse of the physical size of the mask unit aperture.

In addition, the MTF will have contributions from aperture diffraction, MTF_d, and lens aberrations, MTF_l, if present. Diffraction should be less severe for signal-encoding than for source-encoding. Lens aberrations are insignificant at the spatial frequencies reached in our experiments. MTF_l is assumed to be unity for all of the classical monochromatic aberrations. For the Hadamard imager, the modulation transfer function, MTF, is approximated as the product of all contributing terms.

HADAMARD MASKS

The encoding mask is the central element in Hadamard transform methods. Spatial light modulators are an elegant mask technology for spectroscopy in the visible and near-infrared.[14-16] However, currently available spatial light modulators are too delicate for

most source-encoded imaging. Existing spatial light modulator technology does not allow access to the ultraviolet. For these applications, mechanically translated masks remain indispensable. We have employed mechanically translated masks, fabricated as slits milled in brass[1,5] or as photographic positives on high contrast film.[3–5]

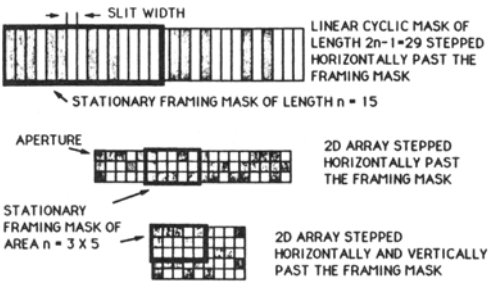

Figure 1. One- and Two-Dimensional Hadamard Mask Systems. Top: 15 element mask arranged for line-encoding; Middle: folded 3 × 5 array, with one axis translation; Bottom: 3 × 5 array folded to use x-axis and y-axis translation.

Several mask arrangements and mask translation schemes are possible. These are shown in Figure 1. The Hadamard masks can be one-dimensional, as in the upper drawing. The Hadamard sequences can be folded to give two dimensional mask sequences requiring only one-dimensional translations. The principle is shown in the center drawing of Figure 1. Here, a 15 element sequence has been folded into three rows of five elements each. The data remains an array of 15 sequential measurements and the data transformation is mathematically the same as in the one-dimensional case.

Alternatively, a folded mask sequence can be shifted in both the x and y directions, as shown in the bottom drawing of Figure 1. This motion requires two translation mechanisms, but can be implemented with a more compact mask. Two-dimensional translation is necessary with 2K element masks to avoid extraordinarily long masks.

There are constraints on the aspect ratios available, if the FHT is required for data transformation. The available aspect ratios depend on the factors of $2^n - 1$. For example, a 255-element mask can be folded into a 15×17 array a 5×51 array or an 3×85 array. In practice the roughly square array will usually be preferred. Curiously, neither a 511 element sequence nor a 2047 element sequence can be folded into approximately square arrays. However, a 1023 element sequence can be folded into a 31×33 array and a 4095 element sequence can be folded into a 45×91 array or a 63×65 array.

Advances in stepping motor and translation stage design have reduced or eliminated many of the disadvantages of mechanical motion. Commercial 10μm step devices provide positioning to within ± 5 μm and can be translated several million inches with no detectable mechanical wear and no missed steps. The largest source of error is thermal expansion of the translation stage lead screw, caused by heat transfer from the motor.

Because the Hadamard masks are used in multiplexing systems, random positioning errors are reduced by $\sqrt{N}$, where N is the number of elements in a Hadamard mask. This factor alone reduces the average error to 0.5 μm or less.[4] The unit aperture of the mask is usually 50–400 μm. The positioning error is 1% or less of this value.

THE MTF OF A SIGNAL-ENCODED HADAMARD IMAGER

The MTF is measured by evaluating the system response to a standard USAF 1951 resolution target supplied as photographic positive on glass. The target contains sets of patterns in spatial frequency increments of $\sqrt[6]{2}$, from 1 line pair per millimeter (lp/mm) to 228 lp/mm.

Our laboratory has introduced the use of transverse photothermal deflection for measurement of transfer functions of source-encoded Hadamard transform imaging systems.[3,4] Colloidal silver photographic positives give strong photothermal signals over a wide range of excitation wavelengths. Our data support the simple resolution model for Hadamard imaging summarized here. Ideally, sampling, that is convolution with the finite area of the aperture, and aperture diffraction, govern the system response.

We have also measured the MTF of a signal-encoded Hadamard microprobe. For these measurements, photothermal techniques are inappropriate. Conventional resolution targets are chromium, silver or aluminum films on quartz or glass and do not not give appreciable Raman or fluorescence signals. The MTF can be measured by encoding the image of a negative target uniformly illuminated from below with a defocused incoherent source, as shown in Figure 2.

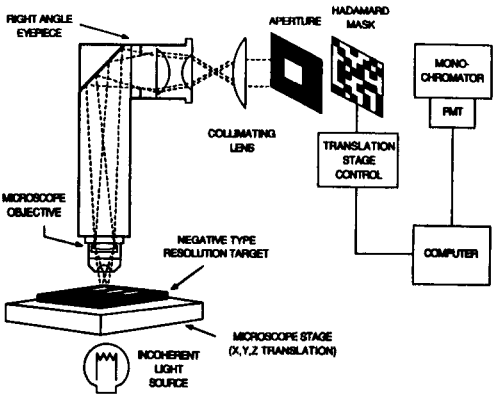

Figure 2. Apparatus for measurement of modulation transfer function of signal-encoded Hadamard imager.

A tungsten bulb beneath a ground glass diffuser serves as the light source. The light coming through the target will behave approximately as Raman scattering originating from the bar patterns. The spectrometer is operated as a monochromator (1-10 cm^{-1} band pass), with a photomultiplier tube.

The system employs a 10× objective, a 10× eyepiece and an 80 mm f.l. collimating lens for an overall magnification of 40×. In this system, the magnification is less then the product of the objective and eyepiece magnifications because of the collimating lens.

Figure 3 is a two-dimensional image of a 3-bar pattern from the resolution target. The bar centers are positioned 13.9 μm apart, which corresponds to a spatial frequency of 71.84 lp/mm. With the 190 μm element mask used in these experiments convolution with the mask unit aperture limits resolution (zero contrast) to 4.8 μm. The Rayleigh diffraction limit is approximately 1 μm. With judicious choice of objective, eyepiece, and mask aperture size there appears to be no theoretical impediment to true diffraction-limited resolution.

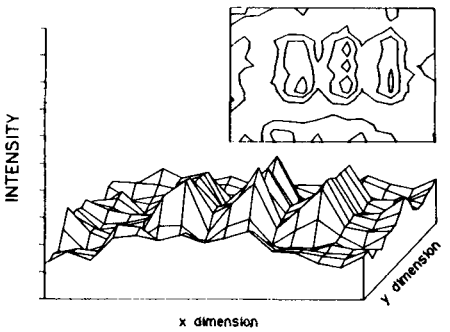

Figure 3. Two-dimensional image of resolution bar target. 40× magnification, 4.8 μm resolution. Target: 71.84 lp/mm. Bar separation: 13.9 μm.

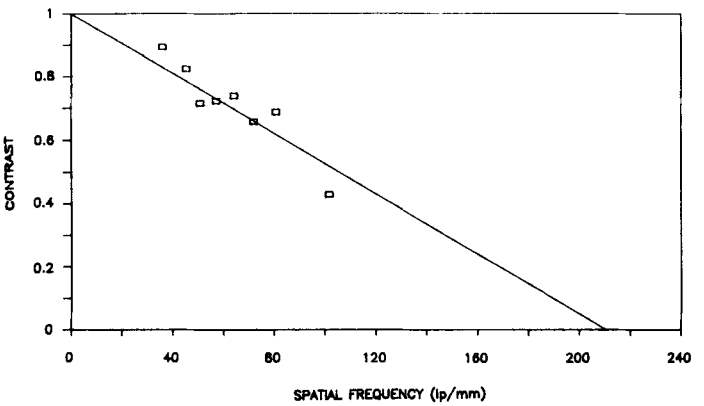

Figure 4. Modulation transfer function of a signal-encoded Hadamard transform microprobe. 40× magnification. Solid line: aperture convolution contribution to MTF.

Figure 4 shows the modulation transfer function for the signal-encoded Hadamard transform microprobe. The solid line represents the theoretical contribution from convolution with the unit aperture. Contrast is measured for cross sections of the two-dimensional image. Good agreement is observed between the measured values and the theoretical prediction. Contributions from aperture diffraction, lens aberrations, and focusing errors are small in this case. To construct a Hadamard imaging system in which diffraction by the microscope objective or aberrations in the microscope optics are resolution limiting, it should only be necessary to decrease the size of the unit aperture or increase the overall magnification of the system.

A SIGNAL-ENCODED HADAMARD RAMAN MICROPROBE

Details of a Hadamard transform Raman microprobe have been described.[8] Figure 5 shows a Raman image of a benzoic acid crystal obtained with this instrument. The apparent crystal dimensions obtained from the Raman image agree well with the directly (reticle) measured dimensions. The intensity scale does not faithfully represent the crystal shape, because illumination and collection efficiency depend on the angles the crystal facets make with the optical system.

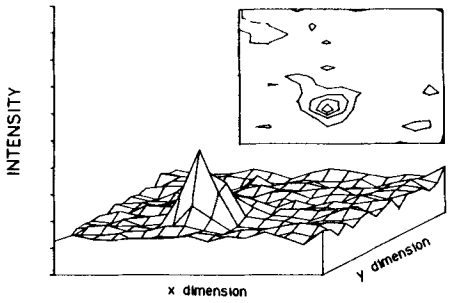

Figure 5. Hadamard transform Raman image of benzoic acid crystal. Excitation: 150 mW, 514.5 nm. Observation at 542 nm (992 cm^{-1}); 10 cm^{-1} spectral resolution; 4.8 μm spatial resolution. 40× magnification.

CONCLUSION

Hadamard transform multiplexing represents a generally useful approach to spatial imaging using intense light sources. The technique is applicable to any linear spectroscopy. Photothermal spectroscopy and other indirect absorption techniques will continue to employ source-encoding. However, Raman scattering and fluorescence imaging will use signal-encoding, to minimize diffraction problems and to enable use of delicate spatial light modulators.

REFERENCES

1. F.K. Fotiou, M.D. Morris, Appl. Spectrosc. **40,** 704 (1986).
2. F.K. Fotiou, M.D. Morris, Anal. Chem. **59,** 185 (1987).
3. F.K. Fotiou, M.D. Morris, Anal. Chem. **59,** 1446 (1987).
4. P.J. Treado, M.D Morris, Appl. Spectrosc. **42,** (in press) (1988).
5. Treado, P.J.; M.D. Morris, Appl. Spectrosc. **42,** 897 (1988).
6. Treado, P.J., M.D. Morris, Appl. Spectrosc. **43,** (in press) (1989).
7. J.J. Blaha, in J.R. Durig, ed. *Vibrational Spectra and Structure, Vol. 10* Elsevier: Amsterdam, 1981, p. 227.
8. G.J. Rosasco in R.J.H. Clark, R.E. Hester, Eds. *Advances in Infrared and Raman Spectroscopy, Vol 10,* Wiley: Chicester, 1981, p. 223.
9. R.M. Hammaker, J.A. Graham, D.C. Tilotta, W.G. Fateley in J. Durig, ed. *Vibrational Spectra and Structure, Vol. 15,* Dekker: New York, 1986, p. 401.
10. W. Stinson, Chem. Engin. News, February 29, 22 (1988).
11. M. Harwit, N.J.A. Sloane, *Hadamard Transform Optics;* Academic Press: New York, 1979.
12. J.W. Goodman, *Introduction to Fourier Optics;* McGraw-Hill: New York, 1968.
13. H.C. Andrews, *Computer Techniques in Image Processing;* Academic Press: New York, 1970.
14. D.C. Tilotta, R.M. Hammaker, W.G. Fateley, Appl. Spectros. **41**, 727 (1987).
15. D.C. Tilotta, R.M. Hammaker, W.G. Fateley, Appl. Opt. **26**, 4825 (1987).
16. D.C. Tilotta, R.D. Freeman, W.G. Fateley, Appl. Spectros. **41**, 1280 (1987).